

Article

Effect of Irradiation with Low-Energy He²⁺ Ions on Degradation of Structural, Strength and Heat-Conducting Properties of BeO Ceramics

Maxim V. Zdorovets ^{1,2,3} , Dmitriy I. Shlimas ^{1,2}, Artem L. Kozlovskiy ^{1,4,*}  and Daryn B. Borgekov ^{1,2}

¹ Laboratory of Solid State Physics, The Institute of Nuclear Physics, Almaty 050032, Kazakhstan; mzdorovets@inp.kz (M.V.Z.); shlimas@mail.ru (D.I.S.); borgekov@mail.ru (D.B.B.)

² Engineering Profile Laboratory, L.N. Gumilyov Eurasian National University, Nur-Sultan 010008, Kazakhstan

³ Department of Intelligent Information Technologies, Ural Federal University, 620075 Yekaterinburg, Russia

⁴ Institute of Geology and Oil and Gas Business, Satbayev University, Almaty 050032, Kazakhstan

* Correspondence: kozlovskiy.a@inp.kz; Tel./Fax: +7-7024413368

Abstract: The paper is devoted to the study of radiation-induced damage kinetics in beryllium oxide ceramics under irradiation with low-energy helium ions with fluences of 10¹⁵–10¹⁸ ion/cm². It was revealed that at irradiation fluences above 10¹⁷ ion/cm², a decrease in radiation-induced damage formation and accumulation rate is observed, which indicates the saturation effect. At the same time, the main mechanisms of structural changes caused by irradiation at these fluences are amorphization processes and dislocation density increase, while at fluences of 10¹⁵–10¹⁶ ion/cm², the main mechanisms of structural changes are due to the reorientation of crystallites and a change in texture, with a small contribution of crystal lattice distorting factors. It was discovered that the radiation-induced damage accumulation as well as an implanted helium concentration increase leads to the surface layer destruction, which is expressed in the ceramic surface hardness and wear resistance deterioration. It was determined that with irradiation fluences of 10¹⁵–10¹⁶ ion/cm², the decrease in thermal conductivity is minimal and is within the measurement error, while an increase in the irradiation fluence above 10¹⁷ ion/cm² leads to an increase in heat losses by more than 10%.

Keywords: beryllium oxide; helium swelling; radiation defects; low-energy ions; inert matrices



Citation: Zdorovets, M.V.; Shlimas, D.I.; Kozlovskiy, A.L.; Borgekov, D.B. Effect of Irradiation with Low-Energy He²⁺ Ions on Degradation of Structural, Strength and Heat-Conducting Properties of BeO Ceramics. *Crystals* **2022**, *12*, 69. <https://doi.org/10.3390/cryst12010069>

Academic Editors: Linghang Wang and Gang Xu

Received: 19 December 2021

Accepted: 3 January 2022

Published: 5 January 2022

Publisher's Note: MDPI stays neutral with regard to jurisdictional claims in published maps and institutional affiliations.



Copyright: © 2022 by the authors. Licensee MDPI, Basel, Switzerland. This article is an open access article distributed under the terms and conditions of the Creative Commons Attribution (CC BY) license (<https://creativecommons.org/licenses/by/4.0/>).

1. Introduction

In the light of recent developments in nuclear power and alternative energy in energy-intensive countries, particular attention is being paid to the development of technologies using new types and concepts of nuclear fuel use. One such concept is the concept of replacing traditional fuel elements with inert matrices that use plutonium or americium instead of uranium [1–3]. The increased interest in these types of materials is due to the fact that, during their operation, actinides or plutonium are not formed, and the concentration of actinides in spent fuel is significantly lower than in conventional fuel elements or mixed oxide fuel [4–7]. At the same time, the transition of nuclear reactors to the use of plutonium fuel with an inert matrix that does not contain uranium makes it possible to increase the burnup of plutonium by a factor of 2–3, which is one of the main advantages of these materials. Generally, oxide ceramics such as ZrO₂, MgAl₂O₄, CeO₂, and BeO are used as inert matrix materials, interest in which is due to their high resistance to external influences, including heating and mechanical pressure or friction [8–10]. At the same time, one of the key problems in the use of inert nuclear fuel matrices in comparison with traditional fuel elements or mixed oxide fuel is the confirmation of the stability of these materials for long-term operation (more than 10–15 years) and the preservation of strength, mechanical, and heat-conducting properties [9,10].

One of the promising materials for inert oxide-based matrices is beryllium oxide (BeO) ceramics, which has a number of unique physicochemical, heat-conducting, and mechanical

properties [11,12]. The interest in this class of materials is due to its inertness to most types of aggressive media and the ability to work at high temperatures, as well as good absorbing capacity and high thermal conductivity. All this allows us to use these ceramics as neutron reflectors or absorbers, various types of structural materials, etc. [13–15]. It is worth noting that despite the increase in interest in BeO ceramics in recent years, this type of ceramics has been used for a long time as a basis for dosimeters and OSL sensors designed to register ionizing radiation and control the dose load [16–19]. Interest in this area is due to high sensitivity and luminescence properties of beryllium oxide, which allows high accuracy of recording and further determination of radiation dose [16–19]. Moreover, an important area of research in radiation materials science is the study of the applicability and efficiency of doping with beryllium oxide or other rare earth elements of radiation-resistant ceramics and glasses [20–24]. These studies are based on an assessment of the possibility of an increase in the resistance of materials to radiation damage and accumulated defects in the structure, which can lead to disordering and deformation of the material. The main feature of doping in this case is the possibility of increasing stability due to substitution and interstitial processes, as well as the absorbing capabilities of rare earth elements or beryllium oxide, which leads to a slowdown in the accumulation of defects in the structure and subsequent deformation.

At the same time, as it was established earlier, ceramics based on beryllium oxide are highly resistant to radiation damage and the accumulation of radiation-induced defects, which opens up the possibility of their operation for a long time [25,26], while high absorption capacity indices make it possible to use them in fields of increased background radiation or large neutron fluxes.

One of the mechanisms of radiation-induced damage arising in materials used as inert matrices of nuclear fuel or structural materials is the accumulation of implanted or transmutation helium in the structure of the surface layer of ceramics [27–29]. The presence of poorly soluble and, at the same time, highly mobile helium in the structure of the surface layer can lead to its agglomeration, followed by the formation of gas-filled bubbles [30–32]. The formation of such bubbles in the structure of the surface layer of a ceramic or metal can lead to destructive processes of swelling and peeling of the surface layer, which in turn leads to destruction and deterioration of the properties of the material [33,34]. Furthermore, an important factor affecting the working and heat-conducting properties of ceramics is a decrease in the amount of heat removal from the system due to the destruction and destabilization of the properties of the heat-conducting material. The formation of distortions in the structure as a result of the accumulation of gas-filled bubbles can lead to a decrease in the thermal conductivity coefficient, which will lead to destabilization of heat removal from the system, as well as its overheating. From a mechanical point of view, the formation of additional distortions in the near-surface layer of ceramics can lead to a change in its strength and wear resistance, which also has a negative effect on the mode and time of operation.

At the same time, in the case of using oxide ceramics as materials of inert matrices or structural materials in nuclear power, the key factor in their application is knowledge of the kinetics and mechanisms of the degradation of structural, mechanical, and heat-conducting properties, depending on the degree of the accumulation of radiation-induced damage and the subsequent amorphization processes or disordering [35,36]. In this regard, the acquisition of any new data on radiation damage and their effect on change in the properties of ceramics is very significant and relevant today, which prompts a large number of scientific groups to engage in such studies. Based on the foregoing, the key goal of this article is to assess the effect of helium irradiation at doses of 10^{15} – 10^{18} ion/cm² on the change in the mechanical, structural, and heat-conducting properties of BeO ceramics. Interest in this topic is not only due to the possibility of obtaining new data on the radiation resistance of these ceramics, but also due to the assessment of radiation-induced defects and the implanted helium concentration effect on thermal conductivity of ceramics. As is known from the literature, at doses above 10^{17} ion/cm² in the structure of oxide and nitride ceramics, the formation of gas-filled bubbles arising as a result of agglomeration

and filling of helium-implanted voids in the ceramics structure is observed, which leads to its swelling and destruction [37–39]. However, there are still questions associated with the subsequent accumulation of helium when these radiation doses are exceeded, as well as a change in the rate of accumulation of defects and destruction of the material when the effect of saturation with defects occurs.

2. Experimental Part

Ceramics based on beryllium oxide obtained by hot pressing and having a high density (3.018 g/cm^3) close to the reference value (3.020 g/cm^3) were chosen as the samples under study. The original samples were purchased from a commercial company Berlox[®] (American Beryllia Inc., Haskell, NJ, USA) that is engaged in the production of ceramics for commercial and research purposes.

The samples were irradiated at a DC-60 heavy ion accelerator (INP ME RK, Nur-Sultan, Kazakhstan). Low-energy He^{2+} ions with an energy of 40 keV (20 keV/charge) at an ion flux density of $10^{10} \text{ ions/cm}^2\cdot\text{s}$ were used as incident ions. In order to avoid overheating of the samples during irradiation, special water-cooled target holders were used, which made it possible to maintain the temperature of the samples in the range of 30–50 °C, thereby excluding the effect of high-temperature annealing of defects during irradiation. The irradiation fluences were 10^{15} – 10^{18} ion/cm^2 , the choice of which is due to the possibility of simulating the structure swelling effects as a result of ion implantation and helium accumulation in the structure of the surface layer [37–39].

Figure 1 shows the simulation results of radiation damage and the implantation of helium ions in the structure of an irradiated ceramic layer with a depth of 400 nm. The maximum displacement value for fluences of 10^{17} ion/cm^2 – 10^{18} ion/cm^2 is 3–17 dpa, which, in comparison with radiation damage caused by neutron irradiation in the case of oxide ceramics, is 0.3 – $1.7 \times 10^{22} \text{ neutron/cm}^2$. This atomic displacements value for the maximum irradiation fluences is due to the fact that the main contribution to the formation of radiation-induced defects is made by the energy losses of incident He^{2+} ions during interaction with nuclei, while the energy losses on the electron shells value is an order less than the nuclear losses value. According to calculations, the energy losses of incident ions on the nuclei are $182.4 \text{ keV}/\mu\text{m}$, and losses on electron shells are $10.7 \text{ keV}/\mu\text{m}$. In this case, the maximum damage accumulation area is at a depth of 170–300 nm from the surface of the samples, with a maximum at 250–170 nm. The maximum concentration of implanted ions is from 0.1 to 1.3 at.%, for fluences 10^{17} ion/cm^2 – 10^{18} ion/cm^2 .

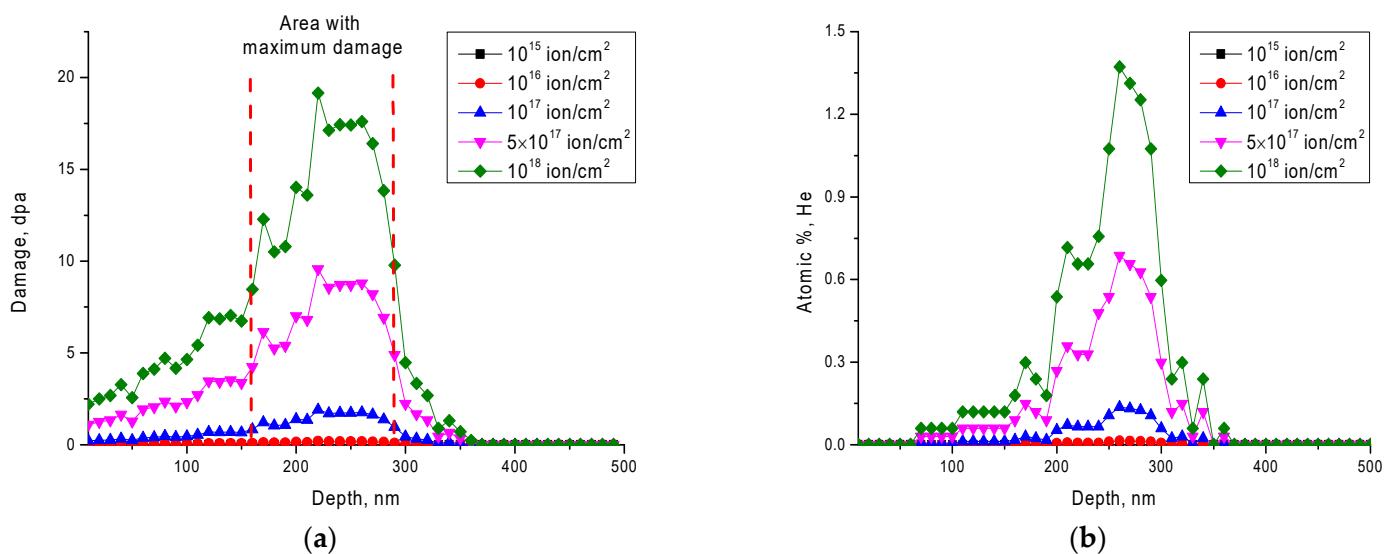


Figure 1. Simulation results for SRIM Pro 2013 [40,41]: (a) Damage vs. depth; (b) Atomic% He vs. depth.

The study of the effect of irradiation and accumulation of radiation-induced defects caused by helium ions on the structural properties and swelling of the crystal lattice was carried out by analyzing the X-ray diffraction patterns of the samples under study before and after irradiation. Diffraction patterns were obtained using a D8 ADVANCE ECO (Bruker, Berlin, Germany) powder diffractometer. Diffraction patterns were recorded in the Bragg-Brentano geometry in the angular range of $2\theta = 35\text{--}75^\circ$, with a step of 0.03° .

The hardness value was determined by the indentation method by using a standard method and using a Vickers pyramid at a load of 500 N. To determine the hardness value and its change as a result of irradiation and radiation-induced defects accumulation, 25 points were measured, which made it possible to determine the standard deviation of the hardness parameters.

The softening degree (*SD*) was determined from the change in the hardness of the near-surface layer before (H_0) and after (H) irradiation, determined by the indentation method using the calculation Equation (1):

$$SD = \left(\frac{H_0 - H}{H_0} \right) \times 100\% \quad (1)$$

The wear resistance of ceramics before and after irradiation was determined by calculating changes in the dry friction coefficient using the tribological method. The number of test cycles was 20,000, and the load on the metal ball was 200 N. Based on the changes in the dry friction coefficient before and after 20,000 test cycles, the value of the coefficient deterioration was determined, which characterizes the loss of the wear resistance of the initial and irradiated materials to mechanical stress.

The determination of the effect of irradiation and subsequent radiation-induced defects accumulation and implanted helium concentration on the heat-conducting properties and a decrease in thermal conductivity was carried out using the standard method for determination of the longitudinal heat flux. This method was implemented using the KIT-800 device (Granat, Moscow, Russia).

3. Results and Discussion

Figure 2 shows the X-ray phase analysis data reflecting changes in the structural parameters of the samples under study depending on the irradiation fluence. According to the data of X-ray phase analysis, it was found that the samples under study have a hexagonal structure with the spatial system P63mc(186) and crystal lattice parameters $a = 2.66986 \text{ \AA}$, $c = 4.33690 \text{ \AA}$. Analysis of the obtained diffraction patterns showed that in the case of the initial samples, the shape of the diffraction lines, as well as the ratio of the areas of reflections and background radiation, indicate a high degree of ordering of the crystal structure (more than 98%). In this case, for irradiated samples, the main changes in the diffraction patterns shown in Figure 2 are associated with two types of changes.

The first type is associated with a change in the intensities and shape of diffraction peaks, caused by the processes of crushing and recrystallization of grains under the action of irradiation, as well as a change in their orientation [35,36]. The appearance of the effect of reorientation of grains as a result of their mobility under the action of irradiation is evidenced by the fact that, at doses of $10^{15}\text{--}10^{17} \text{ ion/cm}^2$, a change in the intensity of the (100), (002), and (101) reflections is observed, with a clearly observed increase in the intensity of the (002) and (101) reflections. This behavior of changes in the intensities of reflections indicates a reorientation of grains under the action of irradiation, caused by the transfer of the kinetic energy of incident ions into the structure of the irradiated layer, followed by the transformation of kinetic energy into thermal energy. This transformation leads to an increase in the thermal vibrations of atoms in the lattice, as well as local heating of the structure. As a result of such influences, a partial reorientation of crystallites occurs, due to both the processes of mobility and the processes of crushing and subsequent amorphization. It should be mentioned that in the work with similar types of commercial ceramics exposed to helium irradiation, it was assumed that the change in the shape of the (002) reflections at

high irradiation doses may be associated with polymorphic transformations of the BeO-hexagonal \rightarrow BeO-cubic type [36]. Such polymorphic transformations can be caused by the crystal structure disordering and partial amorphization processes, which lead to the formation of impurity inclusions of the cubic phase at high radiation doses. In this case, a detailed analysis of the shape of the diffraction reflection (002) at irradiation doses above 10^{17} ion/cm² revealed a strong asymmetry of the reflection characteristic of the formation of impurity inclusions of the cubic BeO phase, the content of which is no more than 3–5%.

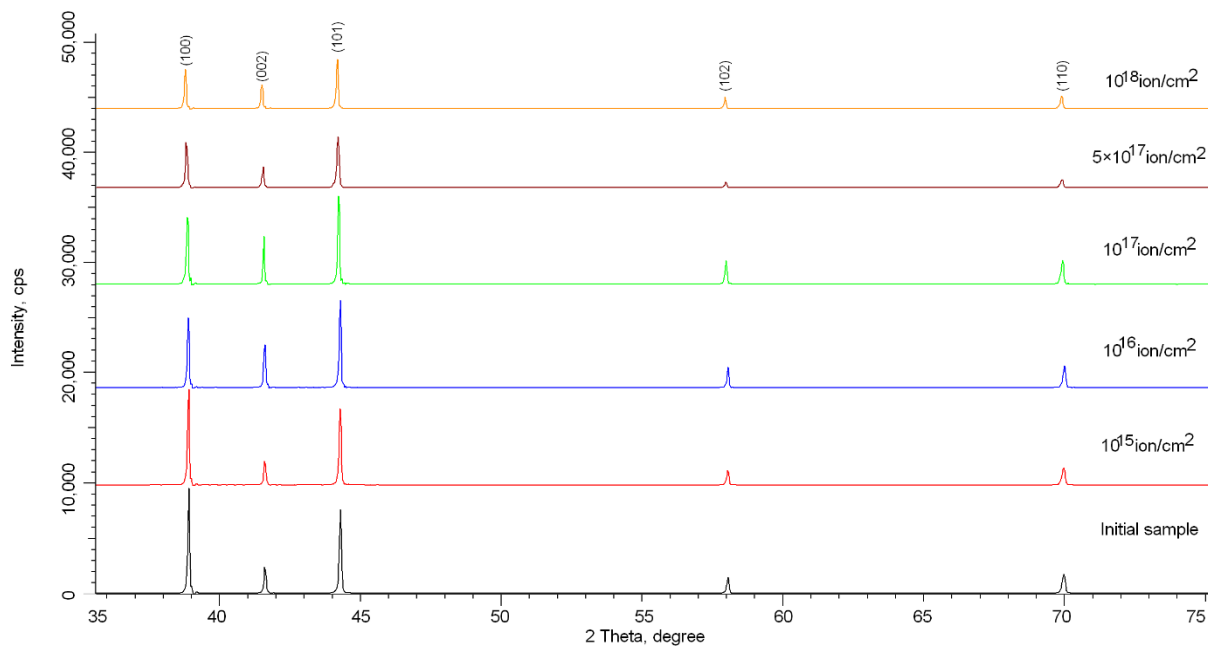


Figure 2. X-ray diffraction patterns of the studied ceramic samples versus irradiation fluence.

The second type of changes is caused by the shift of diffraction maxima to the region of small angles, which indicates crystal lattice deformation and swelling processes under the action of irradiation. A detailed representation of the change in shape and position of the main diffraction lines (100), (002), and (101), reflecting the change in the crystal lattice, is shown in Figure 3a. As can be seen from the presented data, the greatest shift of diffraction reflections is observed for fluences of 10^{16} – 10^{17} ion/cm², while the change in intensities for these fluences is associated only with crystallites reorientation processes and a change in texture. A further increase in the irradiation fluence to 5×10^{17} – 10^{18} ion/cm² leads to a sharp decrease in the intensity of reflections, as well as an increase in the asymmetry of reflections, which, as mentioned above, can be caused by the formation of inclusions of a cubic phase in ceramic structure [37,38]. At the same time, the change in diffraction maxima positions for these irradiation fluences is less pronounced than for lower fluences (see Figure 3b). This behavior may be due to the fact that at these fluences, the dominant radiation damage mechanism is amorphization and the formation of impurity phases in the structure.

Table 1 shows the results of changes in the crystal lattice parameters of the studied ceramics depending on the irradiation fluence. As can be seen from the presented data, an increase in the irradiation fluence leads to a shift in the position of diffraction reflections, and, consequently, a distortion of the crystal lattice leads to an increase in the lattice parameters, as well as its volume. Increase in the crystal lattice volume as a result of irradiation indicates crystal structure swelling due to both deformation and helium ion implantation processes, followed by the formation of gas-filled bubbles in the structure.

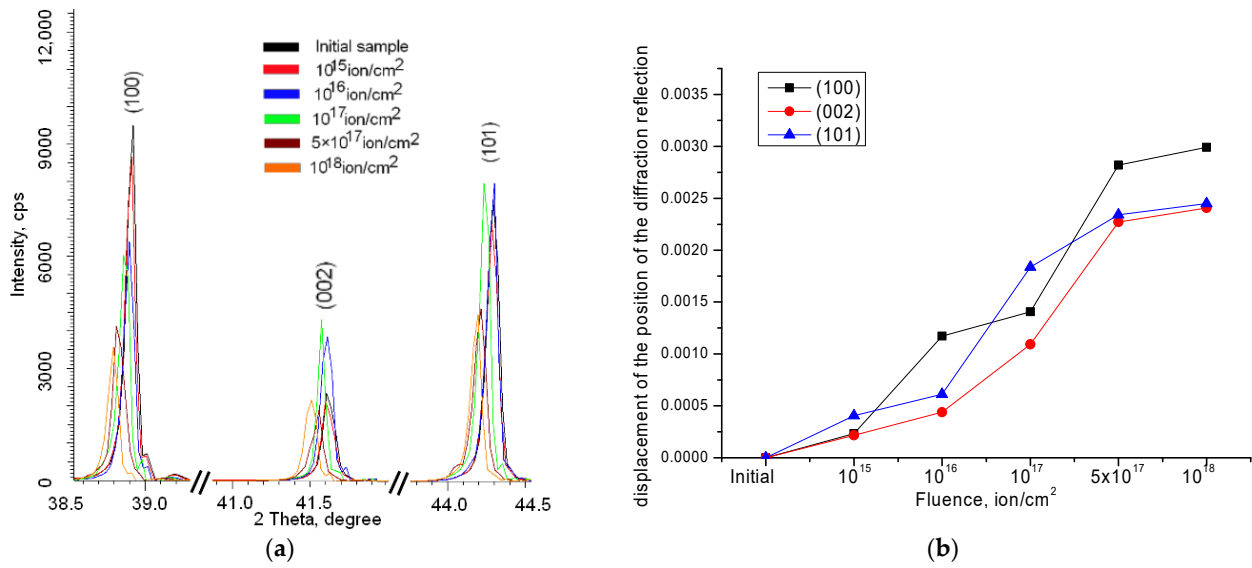


Figure 3. (a) Dynamics of changes in the main diffraction reflections depending on irradiation fluence. (b) Results of change in the shift of diffraction reflections (110), (002), and (101).

Table 1. Crystal lattice data.

Fluence, ion/cm ²	Initial Sample	10 ¹⁵	10 ¹⁶	10 ¹⁷	5 × 10 ¹⁷	10 ¹⁸
Lattice parameter, Å	a = 2.66986, c = 4.33690	a = 2.67039, c = 4.33730	a = 2.67100, c = 4.33966	a = 2.67312, c = 4.34139	a = 2.67678, c = 4.34485	a = 2.67785, c = 4.34658
c/a	1.6243	1.6242	1.6247	1.6241	1.6232	1.6231
Lattice volume, Å ³	26.77	26.79	26.81	26.87	26.96	26.99

Figure 4 shows the results of crystal lattice swelling determined according to Equation (2):

$$Swelling = \left(\frac{V - V_0}{V_0} \right) \times 100\% \tag{2}$$

where V and V_0 are values of the crystal lattice volume for irradiated and initial samples.

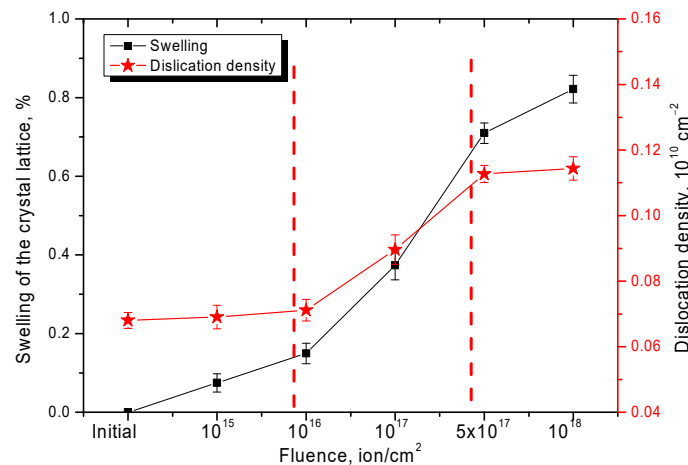


Figure 4. Swelling of the crystal lattice and changes in the dislocation density in the ceramic structure.

The dislocation density in our case was estimated by the standard method based on a change in the size of crystallites, which are estimated from X-ray data [36,37]. The following Equation (3) is used as a calculation formula:

$$\text{Dislocation_density} = \frac{1}{D^2}, \quad (3)$$

where D is the crystallite size determined from the analysis of X-ray diffraction patterns.

As can be seen from the data presented, the change in crystal lattice volume and, consequently, its swelling has a three-stage nature, characterized by different trends in the increase in swelling. At fluences of 10^{15} – 10^{16} ion/cm², the swelling of the crystal lattice is insignificant, which is due to the fact that at these fluences, the main processes caused by irradiation are the processes of reorientation of crystallites and deformation of the structure due to the agglomeration of defects. At the same time, at the given irradiation fluences, changes in dislocation density are also insignificant.

The second stage of swelling changes is associated with a sharp change in the swelling trend and an increase in swelling from 0.15% to 0.7%. The swelling of the crystal lattice at these fluences is primarily associated not only with deformation processes, but also with the accumulation of implanted helium, which leads to the formation of defect agglomerates. In this case, a 1.5-fold increase in the dislocation density is also observed, which indicates a decrease in the grain size as a result of crushing and amorphization.

The third stage of changes is typical for fluences 5×10^{17} – 10^{18} ion/cm² and is characterized by small changes in the swelling and dislocation density, which indicates a decrease in the rate of defect accumulation in the structure and the so-called saturation effect. Moreover, a decrease in the swelling rate can be due to the formation of impurity inclusions in the structure of a cubic phase, leading to amorphization of the structure.

Some of the important performance characteristics of ceramics are their mechanical and strength properties, as well as the dynamics of their change during irradiation and operation. It is a known fact that, under irradiation with heavy ions with low energies, a hardening of the surface layer is observed [42–44]. This is primarily due to the processes of change in the dislocation density, leading to radiation hardening. However, this effect has a strong dose dependence, and is observed mainly for irradiation doses of 10^{12} – 10^{15} ions/cm², which are characterized by the formation of dislocation and point defects, leading to the formation of a strengthening layer. In our case, the irradiation was carried out with He²⁺ ions, which by their nature have high mobility and low solubility in the structure, leading to the formation of agglomerates in the structure in the form of gas-filled regions and bubbles. At the same time, in our case, the irradiation doses were 10^{15} – 10^{18} ion/cm², which is much higher than the doses typical for observing the hardening effect.

Figure 5 shows the results of changes in the hardness of the near-surface layer of ceramics as a result of the accumulation of radiation-induced damage and implanted ions. With an irradiation fluence of 10^{15} – 10^{16} ion/cm², the change in the hardness indicators is insignificant, and is no more than 1–3%, which indicates a high resistance of materials to radiation-induced damage caused by irradiation. With these fluences, damage accumulates in the structure of the surface layer due to the formation of dislocation and cluster defects, as well as the possible agglomeration of implanted helium into gas-filled bubbles. An increase in the radiation dose to 10^{17} – 5×10^{17} ion/cm² leads to a sharp decrease in hardness indicators and an increase in the softening degree of the near-surface layer from 3% to 13–32%, which is a 5–10-fold decrease in the degree of resistance to softening and embrittlement. This destructive behavior of changes in strength properties is associated with a sharp crystal structure swelling, leading to the rupture of chemical and crystal bonds. The increase in swelling is due to a rise in the implanted helium concentration, which leads to an increase in the volumes of gas-filled bubbles and, consequently, to an increase in internal pressure on the crystal structure. A pressure increase in the crystal structure leads to an increase in deformation and distortions of the crystal lattice, which is also associated with an increase in atomic displacements, leading to disorientation of

the crystal structure and its amorphization. As is known from the literature, radiation doses above 10^{17} ion/cm² are critical for oxide and nitride ceramics, as well as multilayer radiation-resistant coatings, which are associated with the formation of blister inclusions and gas-filled bubbles of various diameters in the structure of the irradiated near-surface layer. The formation of such defects leads to embrittlement and partial destruction of the near-surface layer, which entails a decrease in mechanical and strength characteristics. It is known that the processes of the accumulation of radiation damage in the structure of the surface layer are nonlinear, and at certain doses, a decrease in the degree of radiation damage is observed, which is due to the effect of defect accumulation in the structure and amorphization processes [38,45]. This behavior for selected ceramics is observed at a dose above 5×10^{17} ion/cm², which consists of a sharp change in the trend of the decrease of irradiated ceramic strength properties, as well as the softening and embrittlement of the near-surface layer. This is primarily due to an increase in the degree of the amorphization of the irradiated layer and its swelling due to the accumulation of implanted helium in the structure.

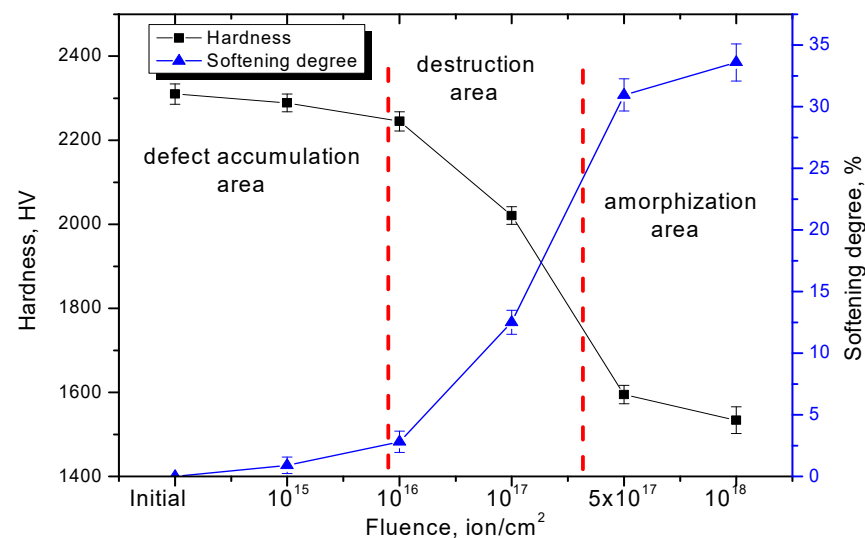


Figure 5. Results of changes in hardness and softening of the ceramic near-surface layer depending on irradiation fluence.

Figure 6 shows the results of the changes in the dry friction coefficient, reflecting the wear resistance of ceramics to external mechanical influences. As can be seen from the data presented, changes in the dry friction coefficient can be divided into two factors, reflecting both wear resistance over a long number of cycles and the change in surface defectiveness as a result of irradiation. At irradiation fluences of 10^{15} – 10^{17} ion/cm², change in the dry friction coefficient is insignificant, which indicates a small degree of surface defectiveness as a result of irradiation and subsequent deformation processes caused by the accumulation of radiation-induced defects in the surface layer structure. The main changes in the dry friction coefficient for these irradiation fluences are observed after 15,000 test cycles, when the coefficient increases by 15–25%, which indicates a surface deterioration and a decrease in wear resistance.

For fluences of 5×10^{17} – 10^{18} ion/cm², an increase in the dry friction coefficient is observed from 0.34 (initial sample) to 0.42 and 0.51, respectively, which indicates a surface deterioration and the formation of additional defects or irregularities leading to an increase in friction resistance. This behavior may be due to the defect accumulation in the structure, as well as partial amorphization, which leads to a sharp deterioration of not only hardness, but also wear resistance. Furthermore, a decrease in resistance to mechanical stress is evidenced by a sharp deterioration in the dry friction coefficient after 15,000 tests, which indicates the low stability of the near-surface irradiated layer to mechanical stress.

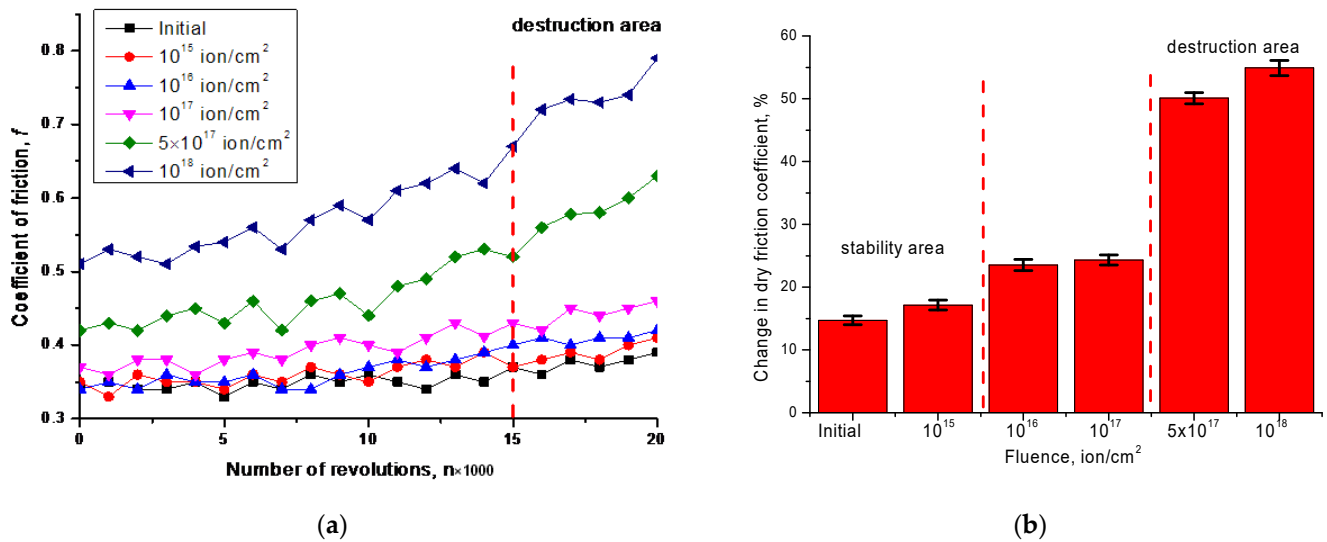


Figure 6. (a) Results of changes in the dry friction coefficient depending on the number of test cycles; (b) Results of dry friction coefficient deterioration depending on irradiation fluence.

Figure 7 shows the results of changes in the heat-conducting properties of ceramics, as well as thermal conductivity loss depending on irradiation fluence and accumulated radiation damage concentration.

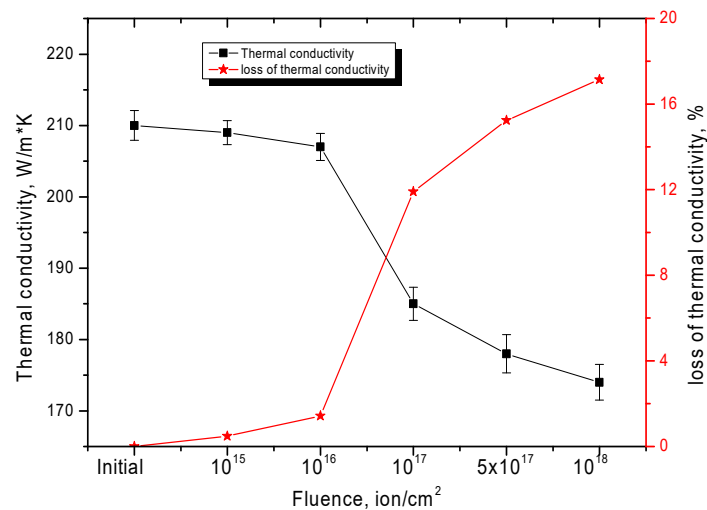


Figure 7. Results of changes in the heat-conducting properties of ceramics before and after irradiation.

The general appearance of the trend in the thermal conductivity coefficient is similar to changes in the strength and structural properties of ceramics, which indicates a direct dependence of the effect of radiation-induced defects concentration in the irradiated near-surface layer structure on the heat-conducting properties. In this case, accumulation of radiation-induced damage, entailing deformation and swelling of the crystal structure, leads to a decrease in heat-conducting properties. However, the formation of impurity inclusions in the structure of the irradiated layer slows down thermal conductivity deterioration. Thus, the obtained dependences of changes in heat-conducting properties indicate that at irradiation doses of 10^{15} – 10^{16} ions/cm², heat losses are no more than 1–2%, which is within acceptable limits. However, the accumulation of radiation-induced defects, as well as the concentration of implanted helium in the structure of the surface layer, leads to sharp thermal conductivity deterioration and significant heat losses exceeding 10% of the initial value.

4. Conclusions

In conclusion, we can summarize the results of the studies carried out aimed at obtaining new information on the radiation resistance of BeO ceramics to the helium swelling processes and subsequent near-surface layer destruction. During research, it was found that the change in structural properties depending on irradiation fluence occurs in two stages associated with different mechanisms of radiation-induced defect accumulation. It was found that at irradiation fluences above 10^{17} ion/cm², the dominant radiation damage mechanism is amorphization and formation of impurity phases in the structure. In turn, the rate and value of the crystal lattice swelling is directly dependent on implanted helium concentration and subsequent partial amorphization and disordering processes of the crystal structure. During the study of changes in the mechanical and strength properties of ceramics depending on irradiation fluence, it was found that the destructive behavior of changes in strength properties is directly related to the crystal structure swelling, as well as the radiation-induced defect accumulation rate. During the study of heat-conducting properties, it was found that with an irradiation fluence of 10^{15} – 10^{16} ion/cm², the decrease in thermal conductivity is minimal and within the measurement error, while an increase in irradiation fluence above 10^{17} ion/cm² leads to an increase in heat loss by more than 10%.

Author Contributions: Conceptualization, M.V.Z., D.I.S., D.B.B. and A.L.K.; methodology, D.B.B., D.I.S. and A.L.K.; formal analysis, M.V.Z.; investigation, D.I.S., A.L.K. and M.V.Z.; resources, M.V.Z.; writing—original draft preparation, review and editing, D.I.S., M.V.Z., D.B.B. and A.L.K.; visualization, M.V.Z.; supervision, M.V.Z. All authors have read and agreed to the published version of the manuscript.

Funding: This research was funded by the Science Committee of the Ministry of Education and Science of the Republic of Kazakhstan (No. AP08855828).

Institutional Review Board Statement: Not applicable.

Informed Consent Statement: Not applicable.

Data Availability Statement: Not applicable.

Conflicts of Interest: The authors declare that they have no conflict of interest.

References

1. Neeft, E.; Bakker, K.; Schram, R.; Conrad, R.; Konings, R. The EFTTRA-T3 irradiation experiment on inert matrix fuels. *J. Nucl. Mater.* **2003**, *320*, 106–116. [[CrossRef](#)]
2. Gong, X.; Ding, S.; Zhao, Y.; Huo, Y.; Zhang, L.; Li, Y. Effects of irradiation hardening and creep on the thermo-mechanical behaviors in inert matrix fuel elements. *Mech. Mater.* **2013**, *65*, 110–123. [[CrossRef](#)]
3. Zhang, J.; Wang, H.; Wei, H.; Tang, C.; Lu, C.; Huang, C.; Ding, S.; Li, Y. Modelling of effective irradiation swelling for inert matrix fuels. *Nucl. Eng. Technol.* **2021**, *53*, 2616–2628. [[CrossRef](#)]
4. Korneeva, E.; Ibrayeva, A.; van Vuuren, A.J.; Kurpaska, L.; Clozel, M.; Mulewska, K.; Kirilkin, N.; Skuratov, V.; Neethling, J.; Zdorovets, M. Nanoindentation testing of Si₃N₄ irradiated with swift heavy ions. *J. Nucl. Mater.* **2021**, *555*, 153120. [[CrossRef](#)]
5. Luzzi, L.; Barani, T.; Boer, B.; Cognini, L.; Del Nevo, A.; Lainet, M.; Lemehov, S.; Magni, A.; Marelle, V.; Michel, B.; et al. Assessment of three European fuel performance codes against the SUPERFACT-1 fast reactor irradiation experiment. *Nucl. Eng. Technol.* **2021**, *53*, 3367–3378. [[CrossRef](#)]
6. Xiang, F.; He, Y.; Niu, Y.; Deng, C.; Wu, Y.; Wang, K.; Tian, W.; Su, G.; Qiu, S. A new method to simulate dispersion plate-type fuel assembly in a multi-physics coupled way. *Ann. Nucl. Energy* **2022**, *166*, 108734. [[CrossRef](#)]
7. Boer, B.; Lemehov, S.; Wéber, M.; Parthoens, Y.; Gysemans, M.; McGinley, J.; Somers, J.; Verwerft, M. Irradiation performance of (Th,Pu)O₂ fuel under Pressurized Water Reactor conditions. *J. Nucl. Mater.* **2016**, *471*, 97–109. [[CrossRef](#)]
8. Sarma, K.; Fourcade, J.; Lee, S.-G.; Solomon, A. New processing methods to produce silicon carbide and beryllium oxide inert matrix and enhanced thermal conductivity oxide fuels. *J. Nucl. Mater.* **2006**, *352*, 324–333. [[CrossRef](#)]
9. Klaassen, F.; Bakker, K.; Schram, R.; Meulekamp, R.K.; Conrad, R.; Somers, J.; Konings, R. Post irradiation examination of irradiated americium oxide and uranium dioxide in magnesium aluminate spinel. *J. Nucl. Mater.* **2003**, *319*, 108–117. [[CrossRef](#)]
10. Lamontagne, J.; Béjaoui, S.; Hanifi, K.; Valot, C.; Loubet, L.; Valot, C. Swelling under irradiation of MgO pellets containing americium oxide: The ECRIX-H irradiation experiment. *J. Nucl. Mater.* **2011**, *413*, 137–144. [[CrossRef](#)]
11. Revankar, S.T.; Zhou, W.; Chandramouli, D. Thermal Performance of UO₂-BeO Fuel during a Loss of Coolant Accident. *Int. J. Nucl. Energy Sci. Eng.* **2015**, *5*, 1. [[CrossRef](#)]

12. Shelley, A. Neutronic analyses of americium burning U-free inert matrix fuels. *Prog. Nucl. Energy* **2020**, *130*, 103567. [[CrossRef](#)]
13. Zhu, X.; Gao, R.; Gong, H.; Liu, T.; Lin, D.Y.; Song, H. UO₂/BeO interfacial thermal resistance and its effect on fuel thermal conductivity. *Ann. Nucl. Energy* **2021**, *154*, 108102. [[CrossRef](#)]
14. Kiiko, V.S.; Vaispapur, V.Y. Thermal Conductivity and Prospects for Application of BeO Ceramic in Electronics. *Glas. Ceram.* **2015**, *71*, 387–391. [[CrossRef](#)]
15. Akishin, G.P.; Turnaev, S.K.; Vaispapur, V.Y.; Gorbunova, M.A.; Makurin, Y.N.; Kiiko, V.S.; Ivanovskii, A.L. Thermal conductivity of beryllium oxide ceramic. *Refract. Ind. Ceram.* **2009**, *50*, 465–468. [[CrossRef](#)]
16. Jahn, A.; Sommer, M.; Ullrich, W.; Wickert, M.; Henniger, J. The BeOmax system—Dosimetry using OSL of BeO for several applications. *Radiat. Meas.* **2013**, *56*, 324–327. [[CrossRef](#)]
17. Bulur, E.; Saraç, B. Time-resolved OSL studies on BeO ceramics. *Radiat. Meas.* **2013**, *59*, 129–138. [[CrossRef](#)]
18. Altunal, V.; Guckan, V.; Yu, Y.; Dicker, A.; Yegingil, Z. A newly developed OSL dosimeter based on beryllium oxide: BeO: Na, Dy, Er. *J. Lumin.* **2020**, *222*, 117140. [[CrossRef](#)]
19. Yukihara, E. A review on the OSL of BeO in light of recent discoveries: The missing piece of the puzzle? *Radiat. Meas.* **2020**, *134*, 106291. [[CrossRef](#)]
20. Altunal, V.; Guckan, V.; Ozdemir, A.; Yegingil, Z. Radiation dosimeter utilizing optically stimulated luminescence of BeO: Na, Tb, Gd ceramics. *J. Alloys Compd.* **2020**, *817*, 152809. [[CrossRef](#)]
21. Altunal, V.; Guckan, V.; Ozdemir, A.; Can, N.; Yegingil, Z. Luminescence characteristics of Al- and Ca-doped BeO obtained via a sol-gel method. *J. Phys. Chem. Solids* **2019**, *131*, 230–242. [[CrossRef](#)]
22. Wójcik, N.A.; Tagiara, N.S.; Ali, S.; Górnicka, K.; Segawa, H.; Klimczuk, T.; Kamitsos, E.I. Structure and magnetic properties of BeO-Fe₂O₃-Al₂O₃-TeO₂ glass-ceramic composites. *J. Eur. Ceram. Soc.* **2021**, *41*, 5214–5222. [[CrossRef](#)]
23. Aşlar, E.; Meric, N.; Şahiner, E.; Erdem, O.; Kitis, G.; Polymeris, G.S. A correlation study on the TL, OSL and ESR signals in commercial BeO dosimeters yielding intense transfer effects. *J. Lumin.* **2019**, *214*, 116533. [[CrossRef](#)]
24. Altunal, V.; Guckan, V.; Ozdemir, A.; Ekicibil, A.; Karadag, F.; Yegingil, I.; Zydhachevskyy, Y. A systematic study on luminescence characterization of lanthanide-doped BeO ceramic dosimeters. *J. Alloys Compd.* **2021**, *876*, 160105. [[CrossRef](#)]
25. Trukhanov, A.V.; Kozlovskiy, A.L.; Ryskulov, A.E.; Uglov, V.V.; Kislitsin, S.B.; Zdorovets, M.V.; Trukhanov, S.V.; Zubar, T.I.; Astapovich, K.A.; Tishkevich, D.I. Control of structural parameters and thermal conductivity of BeO ceramics using heavy ion irradiation and post-radiation annealing. *Ceram. Int.* **2019**, *45*, 15412–15416. [[CrossRef](#)]
26. Snead, L.; Zinkle, S.; White, D. Thermal conductivity degradation of ceramic materials due to low temperature, low dose neutron irradiation. *J. Nucl. Mater.* **2005**, *340*, 187–202. [[CrossRef](#)]
27. Ryazanov, A.I.; Klaptsov, A.V.; Kohyama, A.; Katoh, Y.; Kishimoto, H. Effect of Helium on Radiation Swelling of SiC. *Phys. Scr.* **2004**, *T111*, 195. [[CrossRef](#)]
28. Ghoniem, N.; Takata, M. A rate theory of swelling induced by helium and displacement damage in fusion reactor structural materials. *J. Nucl. Mater.* **1982**, *105*, 276–292. [[CrossRef](#)]
29. Wang, H.; Qi, J.; Guo, H.; Chen, R.; Yang, M.; Gong, Y.; Huang, Z.; Shi, Q.; Liu, W.; Wang, H.; et al. Influence of helium ion radiation on the nano-grained Li₂TiO₃ ceramic for tritium breeding. *Ceram. Int.* **2021**, *47*, 28357–28366. [[CrossRef](#)]
30. Scaffidi-Argentina, F.; Donne, M.; Ferrero, C.; Ronchi, C. Helium induced swelling and tritium trapping mechanisms in irradiated beryllium: A comprehensive approach. *Fusion Eng. Des.* **1995**, *27*, 275–282. [[CrossRef](#)]
31. Allen, W.; Zinkle, S. Lattice location and clustering of helium in ceramic oxides. *J. Nucl. Mater.* **1992**, *191–194*, 625–629. [[CrossRef](#)]
32. Van Veen, A.; Konings, R.; Fedorov, A. Helium in inert matrix dispersion fuels. *J. Nucl. Mater.* **2003**, *320*, 77–84. [[CrossRef](#)]
33. Su, Q.; Inoue, S.; Ishimaru, M.; Gigax, J.; Wang, T.; Ding, H.; Demkowicz, M.J.; Shao, L.; Nastasi, M. Helium irradiation and implantation effects on the structure of amorphous silicon oxycarbide. *Sci. Rep.* **2017**, *7*, 3900. [[CrossRef](#)]
34. Liu, P.; Xue, L.; Yu, L.; Liu, J.; Hu, W.; Zhan, Q.; Wan, F. Microstructure change and swelling of helium irradiated beryllium. *Fusion Eng. Des.* **2019**, *140*, 62–66. [[CrossRef](#)]
35. Shi, K.; Shu, X.; Shao, D.; Zhang, H.; Liu, Y.; Peng, G.; Lu, X. Helium ions' irradiation effects on Gd₂Zr₂O₇ ceramics holding complex simulated radionuclides. *J. Radioanal. Nucl. Chem.* **2017**, *314*, 2113–2122. [[CrossRef](#)]
36. Kislitsin, S.; Ryskulov, A.; Kozlovskiy, A.; Ivanov, I.; Uglov, V.; Zdorovets, M. Degradation processes and helium swelling in beryllium oxide. *Surf. Coat. Technol.* **2020**, *386*, 125498. [[CrossRef](#)]
37. Kozlovskiy, A.L.; Zdorovets, M.V. Study of the radiation disordering mechanisms of AlN ceramic structure as a result of helium swelling. *J. Mater. Sci. Mater. Electron.* **2021**, *32*, 21658–21669. [[CrossRef](#)]
38. Shlimas, D.I.; Zdorovets, M.V.; Kozlovskiy, A.L. Synthesis and resistance to helium swelling of Li₂TiO₃ ceramics. *J. Mater. Sci. Mater. Electron.* **2020**, *31*, 12903–12912. [[CrossRef](#)]
39. Matsunaga, J.; Sakamoto, K.; Muta, H.; Yamanaka, S. Dependence of vacancy concentration on morphology of helium bubbles in oxide ceramics. *J. Nucl. Sci. Technol.* **2014**, *51*, 1231–1240. [[CrossRef](#)]
40. Ziegler, J.F.; Ziegler, M.D.; Biersack, J.P. SRIM—The stopping and range of ions in matter. *Nucl. Instrum. Methods Phys. Res. Sect. B Beam Interact. Mater. At.* **2010**, *268*, 1818–1823. [[CrossRef](#)]

41. Egeland, G.; Valdez, J.; Maloy, S.; McClellan, K.; Sickafus, K.; Bond, G. Heavy-ion irradiation defect accumulation in ZrN characterized by TEM, GIXRD, nanoindentation, and helium desorption. *J. Nucl. Mater.* **2013**, *435*, 77–87. [[CrossRef](#)]
42. Kadyrzhanov, K.K.; Tinishbaeva, K.; Uglov, V.V. Investigation of the effect of exposure to heavy Xe²²⁺ ions on the mechanical properties of carbide ceramics. *Eurasian Phys. Tech. J.* **2020**, *17*, 46–53. [[CrossRef](#)]
43. Tinishbaeva, K.; Kadyrzhanov, K.K.; Kozlovskiy, A.L.; Uglov, V.V.; Zdorovets, M.V. Implantation of low-energy Ni¹²⁺ ions to change structural and strength characteristics of ceramics based on SiC. *J. Mater. Sci. Mater. Electron.* **2019**, *31*, 2246–2256. [[CrossRef](#)]
44. Jin, K.; Lu, C.; Wang, L.; Qu, J.; Weber, W.; Zhang, Y.; Bei, H. Effects of compositional complexity on the ion-irradiation induced swelling and hardening in Ni-containing equiatomic alloys. *Scr. Mater.* **2016**, *119*, 65–70. [[CrossRef](#)]
45. Li, N.; Fu, E.; Wang, H.; Carter, J.; Shao, L.; Maloy, S.; Misra, A.; Zhang, X. He ion irradiation damage in Fe/W nanolayer films. *J. Nucl. Mater.* **2009**, *389*, 233–238. [[CrossRef](#)]